Cascades of homoclinic orbits to a saddle-centre for reversible and perturbed Hamiltonian systems.

Alan R. Champneys
Department of Engineering Mathematics
University of Bristol
Queen's Building, University Walk
Bristol BS8 1TR, UK

Jörg Härterich
Institut für Mathematik I
Freie Universität Berlin
Arnimallee 2-6
14195 Berlin, Germany

February 4, 1988

Abstract

The bifurcation of double-pulse homoclinic orbits under parameter perturbation is analysed for reversible systems having a homoclinic solution that is biasymptotic to a saddle-centre equilibrium. This is a non-hyperbolic equilibrium with two real and two purely imaginary eigenvalues. Reversibility enforces that small perturbations will not change this eigenvalue configuration. It is found that (generically) an infinite sequence of parameter values exists, on one side of that of the primary homoclinic, for which there are double-pulse homoclinic orbits.

Mielke, Holmes and O'Reilly considered the same situation with the additional assumption of Hamiltonian structure. There, double pulses exist on either both or neither side, depending on a sign condition which also determines whether there can be any recurrent dynamics. It is shown how this sign condition occurs in the purely reversible case, via the breaking of a non-degeneracy assumption. Two possible two-parameter bifurcation diagrams are constructed under the addition of a perturbation that keeps reversibility but destroys Hamiltonian structure.

The results are illustrated by numerical computations on two example systems, one arising as a model for optical spatial solitons in the presence of linear and nonlinear dispersion. These computations agree perfectly with the theory including a different rate at which double pulses accumulate in the Hamiltonian and non-Hamiltonian cases.

AMS Classification Scheme: 34C37, 34C35, 58F14

1 Introduction

Hamiltonian dynamical systems are known to possess special properties, such as persistence of homoclinic orbits and a Liapunov Centre Theorem at elliptic fixed points, that have precise analogies for symmetric trajectories in reversible systems (e.g. [De76]). In this context we take a restrictive definition of a reversible system; an even-order dynamical system being invariant under time reversal and a linear involution that fixes half the phase space variables. A trajectory is termed symmetric if it is invariant under such a transformation as a set. Standard examples are classical Hamiltonian systems with quadratic kinetic energy.

This paper makes a further contribution to the study of the dynamics in a neighborhood of homoclinic orbits to equilibria in autonomous reversible systems, see [Dev77, Här93, Ch94, FT96, Saetal96, Kno97] for other cases and [Ch98] for a review. The assumption here is that the equilibrium (without loss of generality, the origin) is a saddle centre, that is a non-hyperbolic equilibrium having two real and two imaginary eigenvalues. The assumption of reversibility is enough to ensure that such a linearisation will persist under parameter perturbation [De76] (the same would be true under just the assumption of Hamiltonian structure). As argued below (see Figure 2), the existence of symmetric homoclinic orbits in such systems is of codimension one, whereas non-symmetric homoclinic orbits are of codimension three in general, or codim two for Hamiltonian systems (see [Ler91, KL95] for an unfolding of the latter situation). Therefore, it does not affect the codimension of symmetric homoclinic connections whether Hamiltonian structure is present or not. We will analyse only systems of the lowest possible dimension, namely four, for which the phenomenon can occur. Presumably a 'homoclinic centre manifold' theorem as in [San95] can be used to show similar results for higher-dimensional systems.

Of prime concern will be the existence of multi-pulse homoclinic orbits, which are like several copies of the primary seperated by a finite number of small oscillations, for parameter values close to that of the primary. Mielke, Holmes and O'Reilly [MHO92] have analysed this question for reversible Hamiltonian systems, and also the construction of shift dynamics in a neighbourhood of the primary homoclinic orbit. See also the results of [Reg97]. Here we shall consider the effect of relaxing the assumption of Hamiltonian structure, while keeping reversibility. It will be shown that there are both similarities and differences between the Hamiltonian and reversible theories.

We shall restrict our attention to double-pulse homoclinic orbits, but, by analogy with the results of [MHO92], similar statements are likely to hold for general n-pulse ($n > 2$) homoclinic orbits too. We will also not study possible shift dynamics for perturbations of

reversible homoclinic orbits to saddle centres, as this is more subtle than in the Hamiltonian case since one cannot reduce the dynamics to the study of a two-dimensional map. In fact, as in the case of homoclinic orbits to saddle-focus in reversible systems [Här93, Ch94], whether shift dynamics necessarily occur is an open question at present.

The rest of this paper is organised as follows. In the next section we give precise notations and state our main theorems. As a preparation for the proofs, we describe in Section 3 the dynamics in a neighbourhood of the equilibrium in terms of a normal form. Taking as an assumption that the dynamics is C^1 conjugate to this normal form locally, we prove our two main theorems in Sections 4 and 5. In Section 6 we study two examples and perform some numerics to illustrate our results on two example systems. The first system is obtained by adjusting a certain fourth-order equation arising as a continuous limit of a discrete lattice equation to make the corresponding system non-Hamiltonian. The second system has physical motivation as a model for nonlinear optical 'spatial solitons' in the presence of linear and nonlinear dispersion. For both models we provide direct numerical evidence of the distinction between Hamiltonian and non-Hamiltonian cases.

Acknowledgement. We should like to the organisers of the Workshop on Time Reversible Symmetries in Dynamical Systems at the University of Warwick, Dec 1996 at which this work was initiated. We should also like to thank Alexander Mielke (University of Hannover) and Patrick Bonckaert (Limburg University) for discussions on normal forms.

2 The main results

Consider the equation

$$\dot{x} = f(x, \mu), \qquad (x, \mu) \in \mathbf{R}^4 \times \mathbf{R}. \tag{1}$$

We assume

(H1) f is *reversible*, i.e. there is a linear involution R with $\dim(\mathrm{fix}(R)) = 2$ and

$$f(Rx, \mu) = -Rf(x, \mu) \qquad \forall (x, \mu) \in \mathbf{R}^4 \times \mathbf{R}^p \tag{2}$$

An important property of reversible systems is the fact that with $x(t)$ also $Rx(-t)$ is a solution of (1).

Definition *A trajectory is called* symmetric *if it is, as a whole, invariant under the reversing symmetry R.*

Without loss of generality, since (1) is autonomous, for such trajectories we may assume $x(0) \in \mathrm{fix}(R)$. Furthermore, we assume

(H2) 0 is a (symmetric) equilibrium for all μ. The eigenvalues of the linearization $Df(0)$ at $\mu = 0$ are $\pm\alpha, \pm i\omega$.

In this case, the equilibrium 0 is called a *saddle-centre*. Due to reversibility, the spectrum of the linearization at a symmetric equilibrium is always symmetric with respect to 0, see [De76]. This implies that for all small $|\mu|$ there will be the same eigenvalue configuration with a pair $\pm\alpha$ of real and a pair $\pm i\omega$ of purely imaginary eigenvalues. Moreover, the corresponding eigenspaces depend smoothly on μ. Hence for sufficiently small μ, by a linear change of variables which depends smoothly on μ, we may assume that the linearization of f at 0 has the form

$$Df(0) = \begin{pmatrix} \alpha & 0 & 0 & 0 \\ 0 & -\alpha & 0 & 0 \\ 0 & 0 & 0 & -\omega \\ 0 & 0 & \omega & 0 \end{pmatrix} \tag{3}$$

where $\alpha = \alpha(0) > 0$ and $\omega = \omega(0) > 0$.

Since the reversing symmetry R maps the eigenvector corresponding to the eigenvalue $\alpha(\mu)$ onto an eigenvector of $-\alpha(\mu)$ and preserves the eigenspace associated with the eigenvalues $\pm i\omega(\mu)$, we set without restriction (after a possible change of sign of some co-ordinates)

$$R = \begin{pmatrix} 0 & 1 & 0 & 0 \\ 1 & 0 & 0 & 0 \\ 0 & 0 & 0 & 1 \\ 0 & 0 & 1 & 0 \end{pmatrix}. \tag{4}$$

Moreover, we assume that the equation can locally be put into some polynomial normal form. These normal forms are described below in Section 3.

(H3) There is a C^1-diffeomorphism that commutes with R and which, locally near 0, conjugates the vector field to a finite-order normal form.

Homoclinic orbits to the origin with systems of with this linearisation are of codimension one in the topology of smooth reversible systems (see, for example, the proof of Lemma 4 in Section 4 below). Hence we assume

(H4) For $\mu = 0$, there is a symmetric homoclinic orbit $q(t)$ converging to 0 as $t \to \pm\infty$.

The final condition is a non-degeneracy hypothesis that concerns the splitting of the stable and unstable manifolds as the parameter μ is varied. In order to formulate it, recall that there is a Liapunov Centre Theorem for reversible systems [De76, Thm. 8.1]. Hence there

is a smooth two-dimensional centre manifold C, locally tangent to the centre eigenspace of 0, that consist entirely of hyperbolic periodic orbits in a neighbourhood of the origin. Using the normal form result in Section 3 below, this manifold will have well-defined 3-dimensional stable and unstable manifolds $W^{s,u}(C)$. Let Σ^s be a μ-independent Poincaré section that for $\mu = 0$ contains a point, $q(t^*)$ for some $t^* > 0$ sufficiently large, on the primary homoclinic orbit in $W^s_{loc}(0)$. Furthermore let $\gamma(\mu) = W^u_{glob}(0;\mu) \cap \Sigma^s$, such that $\gamma(0) = q(t^*)$, then our non-degeneracy hypothesis is

(H5) The vector $v := \frac{d}{d\mu}\gamma(\mu)$ at $\mu = 0$ intersects $W^s(C) \cap \Sigma^s$ transversally.

This condition is formulated more simply using local co-ordinates in Section 4.

Under the above conditions we have the following bifurcation theorem for 2-homoclinic orbits.

Theorem 1 *Assume* **(H1)-(H5)**. *Then there is a sequence $\mu_1, \mu_2, \mu_3, \ldots$ converging to 0 either from the left or from the right such that at parameter values $\mu = \mu_i$ there is a reversible 2-homoclinic orbit to 0.*

Here an orbit is called *2-homoclinic* if it lies entirely in a tubular neighborhood of the primary homoclinic orbit q and makes exactly two windings in this tubular neighborhood.

Our original motivation was the following observation: Holmes, Mielke & O'Reilly [MHO92] considered a system that satisfies assumptions equivalent to **(H1)-(H4)** but possesses also Hamiltonian structure. Depending on the sign of a certain coefficient s of the quadratic part of the Hamiltonian (see Section 5 below for details) either of the following two cases occurs:

$s < 0$ there are two sequences $\mu_1 < \mu_2 < \mu_3 < \ldots < 0$ and $\hat{\mu}_1 > \hat{\mu}_2 > \hat{\mu}_3 > \ldots > 0$ of parameter values where 2-homoclinic orbits exist. (Moreover, although not of concern here, in a full μ-neighbourhood of 0, there are dynamics conjugate to a shift on infinitely many symbols).

$s > 0$ there is a neighborhood of 0 in parameter space where no recurrent behaviour in a neighborhood of the primary homoclinic orbit q can be found.

This sign condition is formulated in terms of the Hamiltonian, so it seems natural to find either an analogue in the non-Hamiltonian case or to prove that there is some difference between the Hamiltonian and the non-Hamiltonian case. We will do the latter and show below that for Hamiltonian systems condition **(H5)** is never satisfied (in fact, as we will

see in Section 5, the vector v generically lies tangent to $W^s(C)$ in Σ^s). This explains the difference between our Theorem 1 and the results in [MHO92]. We want to emphasize that Theorem 1 shows that without Hamiltonian structure one can generically expect to find infinitely many 2-homoclinic orbits for parameter values near 0.

However, a reversible Hamiltonian system as considered in [MHO92] can be embedded in a one-parameter family of reversible vector fields. To this end we introduce another parameter ν and consider

$$\dot{x} = f(x, \mu, \nu), \qquad (x, \mu, \nu) \in \mathbf{R}^4 \times \mathbf{R} \times \mathbf{R}. \tag{5}$$

Then the following theorem holds:

Theorem 2 *Assume*

(i) Conditions **(H1)-(H4)** *hold for all* ν.

(ii) System (5) is a Hamiltonian system for $\nu = 0$.

(iii) $\frac{d}{d\nu} v = \frac{d^2}{d\mu d\nu}\gamma(\mu, \nu)$ *at* $\mu = \nu = 0$ *is transverse to* $W^s(C) \cap \Sigma^s$.

Then there are infinitely many curves $\nu_i = \nu_i(\mu)$, $i = 1, 2, \ldots$ *that correspond to 2-homoclinic orbits.*

Two cases can be distinguished (compare Figs. 1(a) and (b)) corresponding to the sign of s *for the Hamiltonian system at* $\nu = 0$.

Finally, suppose that system (1) has odd symmetry

(H6) $f(x, \mu) = f(-x, \mu)$.

Then we have that (1) is reversible under $-R$ also, which leads to the following.

Corollary 3 *Assume* **(H1)-(H4)** *and* **(H6)**, *then:*

- *Given* **(H5)**, *then there are two sequences* $\mu_1 < \mu_2 < \mu_3 < \ldots < 0$ *and* $\hat{\mu}_1 > \hat{\mu}_2 > \hat{\mu}_3 > \ldots > 0$ *of parameter values where 2-homoclinic orbits exist. One sequence corresponds to* R*-reversible orbits, the other to* $-R$*-reversible.*

- *Given Hamiltonian structure, then there are two sequences* $\mu_1 < \mu_2 < \mu_3 < \ldots < 0$ *and* $\hat{\mu}_1 > \hat{\mu}_2 > \hat{\mu}_3 > \ldots > 0$ both *corresponding to* S*-reversible 2-homoclinic orbits where* $S = R$ *or* $-R$ *depending on the sign of* s.

- *Given the assumptions of Theorem 2, then the sign of* μ *for which* R*-reversible and* $-R$*-reversible pulses occur is determined by the sign of* ν.

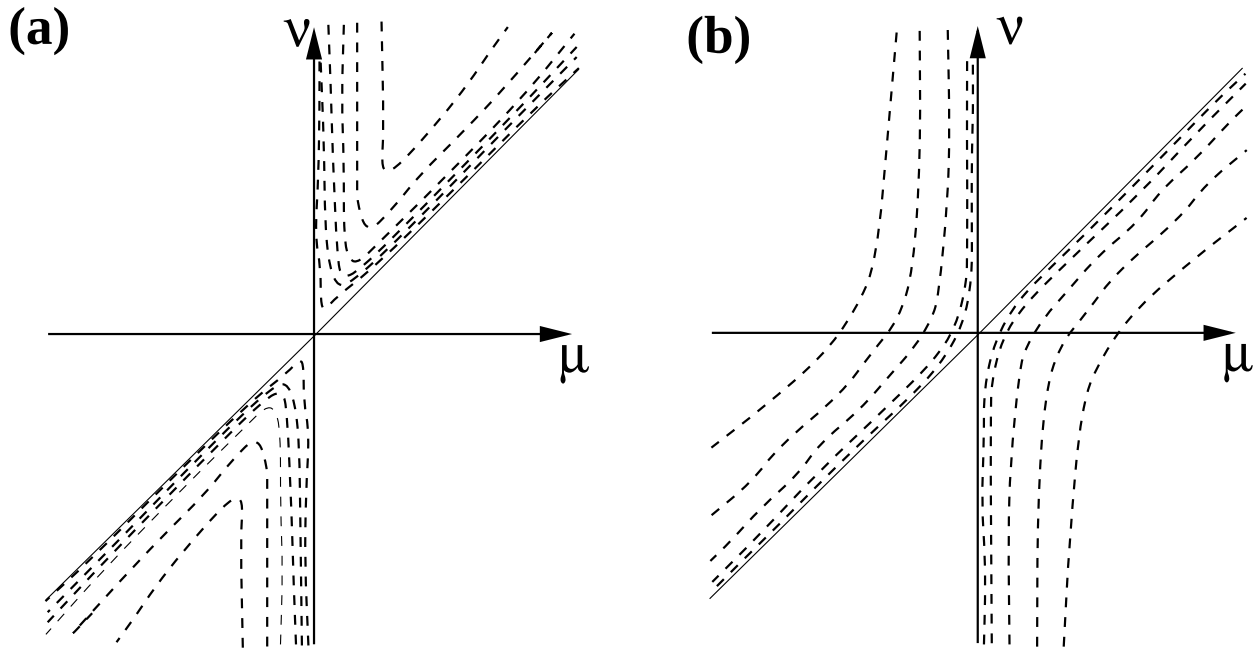

Figure 1: Two-parameter unfolding of 2-pulse homoclinic orbits (dashed lines) in a neighbourhood of a primary homoclinic which occurs for $\mu = 0$. The parameter ν is a generic Hamiltonian-breaking parameter. Cases (a) and (b) correspond respectively to $s > 0$ and $s < 0$ for the Hamiltonian system at $\nu = 0$. The additional solid straight line corresponds to parameter values $\mu = \mu_h(\nu)$ at which heteroclinic orbits exist from the origin to a small amplitude periodic orbit (see Section 5).

3 The normal form

It has become quite standard to simplify a dynamical system near a singular point by using normal form analysis, see for example [Eletal, IA92]. Such a normal form in the case of interest here will be essentially determined by the linear part of f and the reversibility. The procedure is simple. First one calculates the normal form near a saddle-centre equilibrium without taking reversibility into account. The normal form inherits the reversibility of the original vector field. So in a second step we have to check which restrictions are imposed on the already computed normal form. Without the reversibility one arrives at the following $(2n+1)$st-order normal form where P_1, P_2, Q_1 and Q_2 are n-th order polynomials:

$$\dot{x} = \begin{pmatrix} x_1 \cdot P_1(x_1x_2, x_3^2 + x_4^2, \mu) \\ x_2 \cdot P_2(x_1x_2, x_3^2 + x_4^2, \mu) \\ x_4 \cdot Q_1(x_1x_2, x_3^2 + x_4^2, \mu) \\ x_3 \cdot Q_2(x_1x_2, x_3^2 + x_4^2, \mu) \end{pmatrix}. \tag{1}$$

Taking into account the reversibility, gives the additional restriction

$$P_1 = -P_2 \quad , \quad Q_1 = -Q_2.$$

Hence one arrives at the following $(2n+1)$-st order normal form:

$$\dot{x} = \begin{pmatrix} x_1 \cdot P(x_1x_2, x_3^2 + x_4^2, \mu) \\ -x_2 \cdot P(x_1x_2, x_3^2 + x_4^2, \mu) \\ -x_4 \cdot Q(x_1x_2, x_3^2 + x_4^2, \mu) \\ x_3 \cdot Q(x_1x_2, x_3^2 + x_4^2, \mu) \end{pmatrix} \tag{2}$$

with P and Q being real n-th order polynomials and $P(0,0,\mu) = \alpha(\mu), Q(0,0,\mu) = \omega(\mu)$. Note that this normal form is integrable: it possesses the first integrals $I_1 := x_1x_2$ and $I_2 := x_3^2 + x_4^2$.

It is not known whether any vector field locally near a reversible saddle-center can be conjugated to such a normal form. The Liapunov Centre Theorem for reversible systems guarantees the existence of a two-dimensional centre manifold, but this is not enough. In general, only higher order terms in the "hyperbolic" directions x_1, x_2 can be removed, see e.g. [Sam83, Bon97]. Hence, the resulting normal normal form is more complicated and it is not even clear that the conjugating diffeomorphism commutes with the action of R. So for the present paper, we take as an assumption that our original vector field is conjugate to the normal form (2).

Note also that, for the normal form (2), the local unstable and stable manifolds of 0 are just the x_1- and x_2-axis. The local center manifold C is filled with circular periodic orbits and its stable manifold $W^s(C) = \{x_2 = 0\}$ is independent of μ.

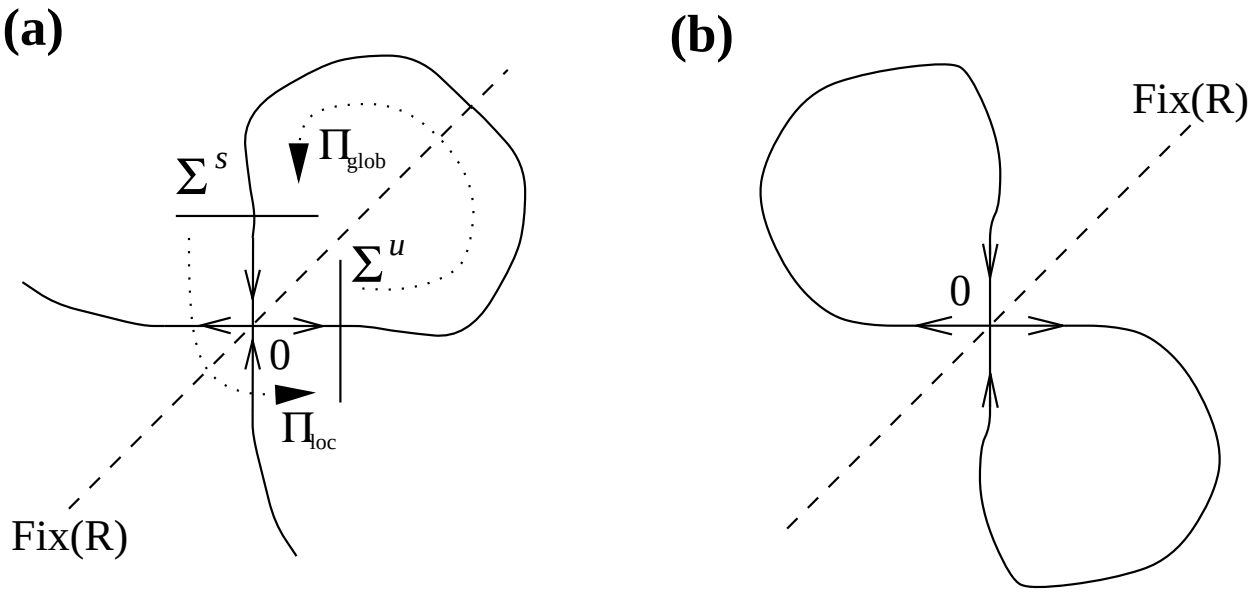

Figure 2: (a) The maps Π_{loc} and Π_{glob} in a neighbourhood of a symmetric homoclinic orbit. The figure is drawn by projecting out the two co-ordinate directions corresponding to the centre manifold at 0. (b) A possible configuration of non-symmetric homoclinic orbits. By reversibility they must occur in pairs, and since they do not intersect fix(R) they are of a higher co-dimension. Given odd symmetry (**H5**) these orbits would be symmetric under $-R$.

4 Proof of Theorem 1

By **(H3)**, we may use the truncated normal form (2) of the vector field for our calculations. The integrability of the normal form has the nice effect that most calculations are simple and the geometry becomes very clear. The calculations are similar to those of Mielke *et al.*, although through the absence of Hamiltonian structure the geometry is more complicated.

We will consider a Poincaré map along the primary homoclinic orbit $q(t)$. This Poincaré map will be decomposed into a local and a global part where the local part is determined by the normal form near 0 and the global part is modelled by a diffeomorphism. See Figure 2

For the decomposition, we will choose a transverse section Σ^u to the homoclinic orbit q at $\mu = 0$. We take

$$\Sigma^u := \{x_1 = r; x_2^2 + x_3^2 + x_4^2 < \delta^2\}$$

where r and δ are chosen small such that Σ^u is contained in the neighborhood of 0 where the vector field is given by the normal form. As a second transverse section we choose the

mirror image

$$\Sigma^s := R(\Sigma^u) = \{x_2 = r; x_1^2 + x_3^2 + x_4^2 < \delta^2\}.$$

Using those two sections we define a local Poincaré map

$$\begin{aligned} \Pi_{loc}^{\mu} : \Sigma^s &\longrightarrow \Sigma^u \\ (x_1^s, x_3^s, x_4^s) &\longmapsto (x_2^u, x_3^u, x_4^u) \end{aligned}$$

induced by the flow of the normal form (2). A global map

$$\Pi_{glob}^{\mu} : \Sigma^u \longrightarrow \Sigma^s$$

is given by the coordinate transformations near 0 and the global flow along the homoclinic orbit q. We suppress for both Poincaré maps their dependence on the parameter μ when the meaning is obvious.

Due to the existence of the primary homoclinic orbit for $\mu = 0$, we know that Π_{glob}^0 maps $(0,0,0) \in \Sigma^u$ to $(0,0,0) \in \Sigma^s$.

Since, by **(H3)**, the coordinate transformation commutes with R, the global map is R-reversible:

$$\Pi_{glob}^{-1}(Rx) = R\Pi_{glob}(x).$$

The next lemma characterizes 2-homoclinic solutions in terms of the two Poincaré return maps.

Lemma 4 *There exists a symmetric 2-homoclinic orbit at the parameter value $\bar{\mu}$ iff*

$$\Pi_{loc}^{\bar{\mu}} \circ \Pi_{glob}^{\bar{\mu}}(0,0,0) = R \circ \Pi_{glob}^{\bar{\mu}}(0,0,0).$$

Proof of lemma 4: We explain first why in our system we are only interested in symmetric homoclinic orbits. Recall that for reversible systems a Liapunov Centre Theorem holds; the centre manifold is foliated by hyperbolic periodic orbits. For that reason every homoclinic orbit has to lie in the one-dimensional unstable manifold of 0 and, since it is a homoclinic orbit, also in the one-dimensional stable manifold of 0. So the homoclinic orbit *is* (one component of) both the stable and unstable manifold. Since those two manifolds are related by the reversing symmetry R (see [De76]) the homoclinic orbit has either to be symmetric, or there are two symmetry-related homoclinic orbits (as in Fig 2(b)). However, the non-symmetric situation is of codimension-three in general reversible systems because we require two one-dimensional manifolds to be identified in $\mathbf{R}^4$ (it would be codim 2 for Hamiltonian reversible systems). By contrast, symmetric homoclinic orbits occur when

the one-dimensional manifold $W^u(0;\mu)$ intersects the plane $\mathrm{fix}(R)$. This is of codimension one in R^4. Hence, since we are interested in generic phenomena on varying one parameter μ, we look only for symmetric 2-homoclinic solutions. These occur when $W^u(0)$ intersects $\mathrm{fix}(R)$ in a neighbourhood of 0. As $(0,0,0) \in \Sigma^u$ lies on the unstable manifold, for a orbit to be 2-homoclinic the condition

$$\Pi_{glob} \circ \Pi_{loc} \circ \Pi_{glob}(0,0,0) = (0,0,0) \in \Sigma^s$$

has to be satisfied. However, by reversibility **(H1)** the pre-image $\Pi_{glob}^{-1}(0,0,0)$ is the image under R of $\Pi_{glob}(0,0,0)$ which gives exactly the condition stated in the lemma. □

The condition from Lemma 4 can also be written in the form

$$\Pi_{glob}(0,0,0) \in S_{symm}$$

where the set S_{symm} is defined as

$$S_{symm} := \{(x_1^s, x_3^s, x_4^s) \in \Sigma^s; \Pi_{loc}(x_1^s, x_3^s, x_4^s) = R(x_1^s, x_3^s, x_4^s)\}. \tag{1}$$

Using the normal form we can get an accurate description of S_{symm} as follows. Owing to the imaginary eigenvalues, it is more convenient to use polar coordinates instead of x_3 and x_4, hence we set

$$\begin{aligned} x_3 &= \varrho \cos\varphi \\ x_4 &= \varrho \sin\varphi. \end{aligned}$$

In these coordinates the normal form equations read

$$\begin{aligned} \dot{x_1} &= P(I_1, I_2, \mu)x_1 && (2)\\ \dot{x_2} &= -P(I_1, I_2, \mu)x_2 && (3)\\ \dot{\varrho} &= 0 \\ \dot{\varphi} &= Q(I_1, I_2, \mu) \end{aligned}$$

where the ϱ-equation reflects the fact that $I_2 = \varrho^2$ is a first integral and the φ-equation gives the angular velocity of the periodic solutions that foliate the centre manifold of 0.

The 'hyperbolic' equations (2), (3) can be used to calculate the time a trajectory spends in going from Σ^s to Σ^u. Especially, we can now give an expression for Π_{loc} in terms of ϱ and φ. As before, we write ϱ^s, φ^s for the polar coordinates in Σ^s and ϱ^u, φ^u for the coordinates in

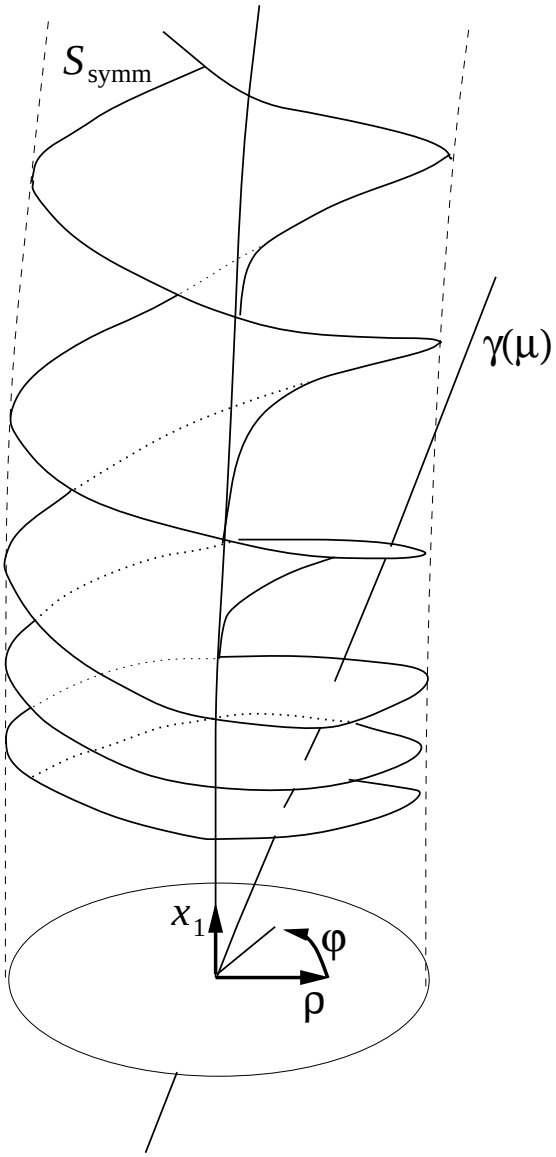

Figure 3: The set S_{symm} for $0 < \varrho < \varrho_{max}$ and $0 < x_1 < x_{max} > 0$, for some $\varrho_{max}, x_{max} < delta$, and its intersection with a generic $\gamma(\mu)$. Decreasing x_1 further than depicted, the double spiral winds faster and faster, with its infinite leaves accumulating on the circle $x_1 = 0$, $\varrho < \varrho_{max}$; which is $W^u(C) \cap \Sigma^s$

Σ^u. Equations (2) and (3) can be solved explicitly since I_1 and I_2 are constants of motion. Then Π_{loc} can be written as

$$\begin{aligned} x_2^u &= x_1^s \\ \varrho^u &= \varrho^s \\ \varphi^u &= \varphi^s + \frac{Q(I_1, I_2, \mu)}{P(I_1, I_2, \mu)} \ln\left(\frac{r}{x_1^s}\right) \end{aligned}$$

A simple calculation shows that the reversing symmetry R leaves ϱ fixed and acts on the φ-coordinate as

$$R\varphi = \frac{\pi}{2} - \varphi.$$

Using this, one gets

$$S_{symm} = \left\{ (x_1^s, \varrho^s, \varphi^s) \in \Sigma^s \ ; \ x_1^s > 0, \frac{\pi}{2} - \varphi^s \equiv \varphi^s + \frac{Q(I_1, I_2, \mu)}{P(I_1, I_2, \mu)} \ln(r/x_1^s) \pmod{2\pi} \right\}. \tag{4}$$

The condition $x_1^s > 0$ is necessary, because orbits with $x_1^s < 0$ leave a neighborhood of 0 not via the section Σ^u but along the other branch of the unstable manifold. In particular, these orbits do not lie in a tubular neighborhood of the primary homoclinic orbit. To get an understanding of Theorem (1), it is useful to visualize the set S_{symm}; see Fig. 3. The intersection of S_{symm} with any of the planes $\{x_1^s = const.\}$ is a curve through $\varrho = 0$ tangent to the line

$$\varphi^s \equiv \frac{\pi}{4} - \frac{\omega}{2\alpha} \ln(r/x_1^s) \pmod{\pi}.$$

Since the ln-term tends to infinity as x_1^s decreases to zero this line rotates infinitely often around $\varrho^s = 0$ as $x_1^s \searrow 0$ to produce the surface S_{symm}. It is easy to verify that the closure of S_{symm} consists of $S_{symm} \cup \{x_1^s = 0\}$. To find the 2-homoclinic orbits, consider now the C^1-curve

$$\gamma(\mu) := \Pi_{glob}^{\mu}(0, 0, 0)$$

that describes how the unstable manifold intersects Σ^s.

We parametrise the curve γ as $(x_1^\gamma(\mu), \varrho^\gamma(\mu), \varphi^\gamma(\mu))$. Then, since in the normal form coordinates $W^s(C) \cap \Sigma^s = \{(x_1^s, \varrho^s, \phi^s) | x_1^s = 0\}$, **(H5)** implies that

$$\frac{d}{d\mu} x_1^\gamma(\mu) \neq 0. \tag{5}$$

We investigate the function

$$\mu \mapsto \Phi(\mu) := \varphi^\gamma(\mu) - \frac{\pi}{4} - \frac{Q(r x_1^\gamma(\mu), \varrho^\gamma(\mu))^2, \mu)}{2P(r x_1^\gamma(\mu), \varrho^\gamma(\mu))^2, \mu)} \ln(r/x_1^\gamma(\mu)). \tag{6}$$

As we have shown, a point of intersection between γ and S_{symm} occurs iff

$$\Phi(\mu) \equiv 0 \ (\mathrm{mod}\, \pi) \text{ and } x_1^\gamma(\mu) > 0.$$

Note first that due to (5), the second condition is satisfied either for all small $\mu > 0$ or for all small $\mu < 0$. Without loss of generality we assume that $x_1^\gamma(\mu) > 0$ for all small positive μ. The existence of infinitely many intersections is then proved if we show that $\Phi(\mu)$ tends to $+\infty$ or $-\infty$ as μ tends to 0 from above. However, this is clear, since $\varphi^\gamma(\mu)$ tends to a limit as $\mu \searrow 0$ and both I_1 and I_2 tend to 0. Hence, the ln-term dominates and, $|\Phi(\mu)| \to \infty$ which completes the proof. □

The proof of the first part of Corollary 3 follows from noticing that

$$S_{-symm} := \{(x_1^s, x_3^s, x_4^s) \in \Sigma^s; \Pi_{loc}(x_1^s, x_3^s, x_4^s) = -R(x_1^s, x_3^s, x_4^s)\} = -S_{symm}.$$

Therefore, for the sign of μ for which $\gamma(\mu)$ does not intersect S_{symm} there will be infinitely many intersections between $\gamma(\mu)$ and $-S_{symm}$. These intersections correspond to $-R$-reversible 2-homoclinic orbits.

The other two parts of the Corollary can be derived similarly from the proof of Theorem 2, which follows. □

5 Proof of Theorem 2

Before we begin with the proof of Theorem 2, we show that assumption **(H5)** fails for Hamiltonian systems:

Lemma 5 *For Hamiltonian reversible systems, the vector*

$$v = \frac{d}{d\mu}|_{\mu=0} \Pi_{glob}^\mu(0,0,0)$$

is always parallel to the plane $\{x_1^s = 0\}$.

Proof : Suppose that (1) may be written in Hamiltonian form with total energy H and canonical co-ordinates q_1, p_1, q_2, p_2, and assume and without loss of generality that 0 is in the zero energy surface $0 \in H_0(\mu) := \{H = 0\}$. Furthermore, suppose that reversibility acts to reverse the momentum variables

$$R : (q_1, p_1, q_2, p_2) \mapsto (q_1, -p_1, q_2, -p_2).$$

Then, locally near 0, the transformation to write (1) in Hamiltonian co-ordinates must take one of the two forms (up to change of sign of all the canonical variables)

$$\begin{pmatrix} q_1 \\ p_1 \\ q_2 \\ p_2 \end{pmatrix} = \begin{bmatrix} 0 & 0 & s & s \\ 0 & 0 & s & -s \\ 1 & 1 & 0 & 0 \\ 1 & -1 & 0 & 0 \end{bmatrix} + \text{ h.o.t.}$$

with $s = \pm 1$ [MHO92]. Therefore, written in the original variables, near 0 the Hamiltonian H has to be of the form

$$H = 2\alpha x_1 x_2 + s\frac{\omega}{2}(x_3^2 + x_4^2) + \text{ h.o.t..} \tag{7}$$

Moreover, when put into normal form (which may now be achieved for any analytical Hamiltonian system by an analytic change of variables — see [MHO92]), then the higher order terms depend only on $x_1 x_2$ and $x_3^2 + x_4^2$ (and μ). If one looks for homoclinic orbits, the set $H_0(\mu) \cap \Sigma^s$ is of importance since $\Pi^{\mu}_{glob}(0,0,0)$ has to lie in $H_0(\mu)$. But, in normal form co-ordinates,

$$H_0 \cap \Sigma^s := \{(x_1, x_2 = r, \varrho, \varphi) \in \Sigma^s \mid 2\alpha r x_1 + \mathcal{O}((r x_1)^2) = -s\frac{\omega}{2}\varrho^2 + \mathcal{O}(\varrho^4)\} \tag{8}$$

which is the equation for a paraboloid tangent to the plane $\{x_1 = 0\}$ at the origin in Σ^s, lying locally entirely in the half-space $s x_1 \leq 0$. In particular, $\Pi^{\mu}_{glob}(0,0,0)$ has to lie tangent to the plane $\{x_1 = 0\}$ at the origin as stated in the Lemma. □

Moreover, the above proof shows that $\gamma(\mu)$ lies on the same side of $\{x_1^s = 0\}$ for all $|\mu|$ small. Thus we conclude that one of the two pictures Fig. 4(a) or (b) applies according to the sign of s.

Now suppose we perturb the Hamiltonian structure in such a way that condition (iii) of Theorem 2 applies. Without loss of generality suppose $\frac{d}{d\nu} v_1 = 1$. Then we have an unfolding as depicted in Fig. 5, which leads to one of the bifurcation diagrams in Fig. 1 depending on the sign of s. Note that the curve $\mu_h(\nu)$ corresponds to parameter values for which the unstable $\Pi^{(\mu,\nu)}_{glob}(0,0,0)$ intersects $x_1^s = 0$ for $\rho > 0$. This corresponds to a heteroclinic connection between the origin and a periodic orbit lying in the centre manifold.

□

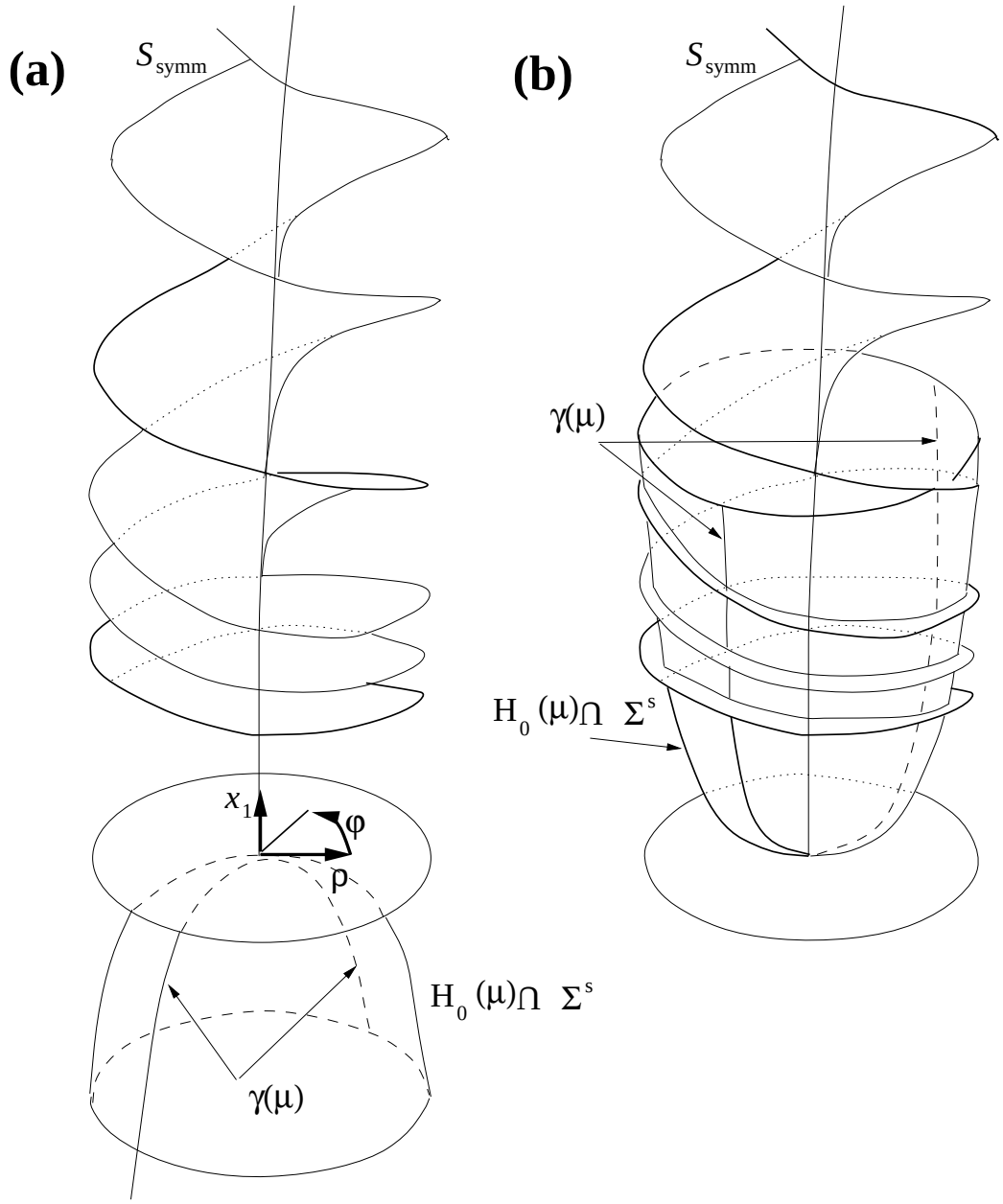

Figure 4: Showing intersections between S_{symm} and $\gamma(\mu)$ for the Hamiltonian case with (a) $s > 0$, and (b) $s < 0$. Depicted similarly to Fig. 3

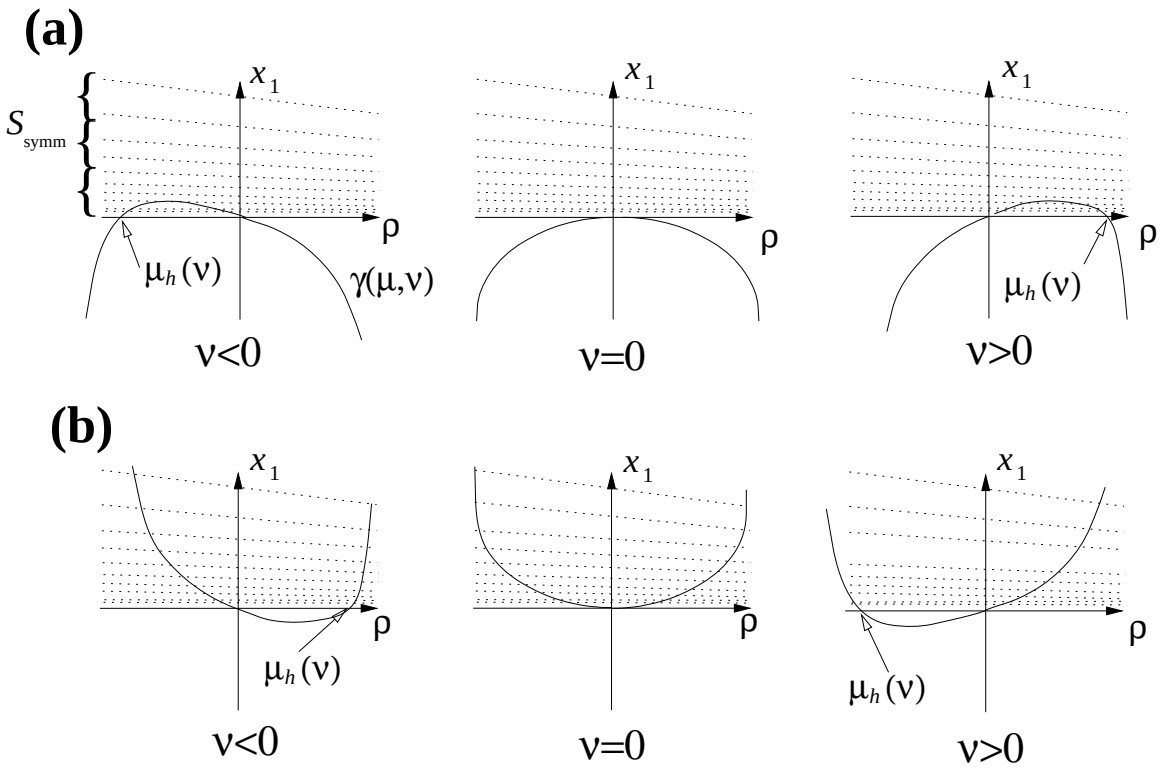

Figure 5: Depicting intersections of $\gamma(\nu, \mu)$ and appropriate slices of S_{symm} (represented by infinitely many disjoint lines), in the two cases (a) $s > 0$, (b) $s < 00$

6 Two examples

We shall illustrate the preceding theory with two examples, the first somewhat artificially generated to suit our purposes, and the second taken from a particular problem in nonlinear optics. In both cases, we do not attempt to verify the non-degeneracy conditions **(H1)**–**(H5)** rigorously. Instead we provide strong *a posteriori* numerical evidence, obtained by direct computation of paths of homoclinic orbits, that the conclusions of Theorems 1 and 2 hold. All numerical computations are based on solving boundary-value problems for homoclinic solutions, see e.g. [Ch98] and references therein. Numerical continuation is performed using the software AUTO [DKK91].

Before presenting the results, we note that we can use the formula (6) to deduce the rate of parameter accumulation of 2-pulses on the primary orbit implied by Theorem 1 in the case of general reversible systems and Theorem 2 for Hamiltonian reversible systems. These rates may be used as additional numerical evidence for the presence or otherwise of Hamiltonian structure.

Theorem 2 shows that there is a sequence of $\{\mu_i\}$ of parameter values at which homoclinic solutions given by $\Phi(\mu) = 0 \pmod{\pi}$ occur. By (6), we have

$$\frac{Q(rx_1^\gamma(\mu_i), \varrho^\gamma(\mu_i)^2, \mu_i)}{2P(rx_1^\gamma(\mu_i), \varrho^\gamma(\mu_i)^2, \mu_i)} \ln(r/x_1^\gamma(\mu_i)) = -\varphi^\gamma(\mu_i) + \frac{\pi}{4} + (n_0 + i)\pi\mathcal{O}(\mu)$$

for some $n_0 \in \mathbb{Z}$. For μ_i sufficiently small (i sufficiently large) this gives

$$\left[-\frac{\omega}{2\alpha} + \mathcal{O}(\mu_i)\right] \ln(r/x_1^\gamma(\mu_i)) = -\varphi^\gamma(0) + \frac{\pi}{4} + (n_0 + i)\pi + \mathcal{O}(\mu_i)$$

which rearranges to

$$x_1^\gamma(\mu_i) = Kr \exp\left(\frac{-2(n_0 + i)\pi\alpha}{\omega} + \mathcal{O}(\mu_i)\right) \tag{9}$$

where $K = \exp[\frac{\alpha}{\omega}(\varphi^\gamma(0) - \frac{\pi}{4})]$.

Now, for general reversible systems satisfying hypothesis **(H5)** we have, by (5),

$$x_1^\gamma(\mu_i) = a\mu_i + \mathcal{O}(\mu_i^2), \tag{10}$$

for some $a \neq 0$. Substituting (10) into (9) for $i = n$ and $i = n + 1$, and dividing, we obtain

$$\frac{\mu_{n+1}}{\mu_n} \to \exp\left(\frac{-2\alpha\pi}{\omega}\right) \quad \text{as } n \to \infty. \tag{11}$$

In the case of a Hamiltonian reversible system, obtained by fixing $\nu = 0$ in the hypothesis of Theorem 2, generically we have

$$x_1^\gamma(\mu_i) = b\mu_i^2 + \mathcal{O}(\mu_i^3),$$

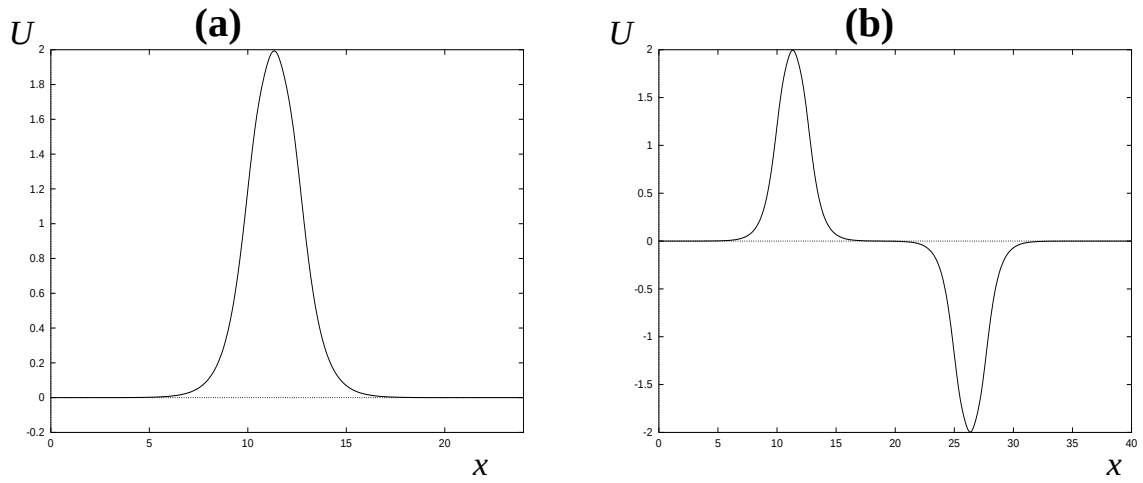

Figure 6: Homoclinic orbits of the Hamiltonian system with $\eta = 0$; (a) primary homoclinic solution at $\lambda^2 = 1.94618\ldots$, (b) a two-pulse homoclinic solution at $\lambda^2 = 1.95220\ldots$.

for some nonzero b. This implies (11) should be replaced by

$$\frac{\mu_{n+1}}{\mu_n} \to \exp\left(\frac{-\alpha\pi}{\omega}\right) \quad \text{as } n \to \infty \tag{12}$$

for Hamiltonian reversible systems.

6.1 A fourth-order equation

The equation

$$\frac{1}{12}v'''' + v'' + \lambda^2 v + v^3 + \frac{3}{4}v(vv'' + (1+\eta)v'^2) = 0 \tag{13}$$

with $\eta = 0$ arises in the continuous limit of a discrete lattice equation known to possess 'up-down' localised breather solutions. See Kivshar *et al.* [KCCB97] for more details.

When $\eta = 0$ there are a choice of variables that put (13) into Hamiltonian form with total energy

$$H = \frac{\lambda^2}{2}u^2 + \frac{1}{2}u'^2 - \frac{1}{24}(u'')^2 - \frac{1}{4}u^4 + \frac{3}{4}u^2u'^2.$$

The addition of the extra parameter η breaks the Hamiltonian structure of this equation. We should remark, however, that we are not aware that η corresponds to anything physical in this model.

For all values of η and λ^2, Equation (13), when viewed as a dynamical system in phase space variables (u, u', u'', u'''), has odd symmetry and is reversible under

$$R : (u, u', u'', u''') \to (u, -u', u'', -u''')$$

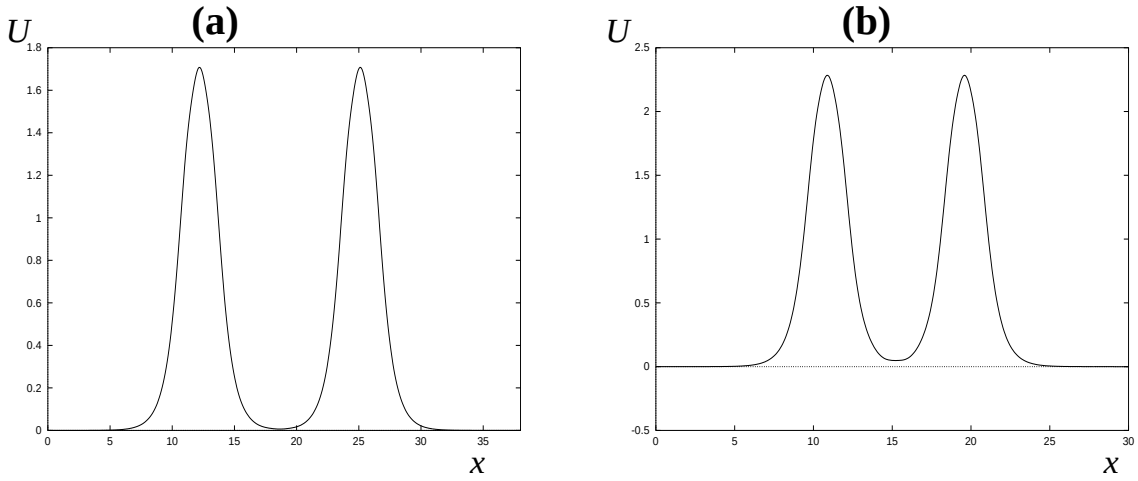

Figure 7: R-symmetric homoclinic orbits of the non-Hamiltonian system with $\eta \neq 0$; (a) at $\eta = 0.5$, $\lambda^2 = 1.571219\ldots$, (b) at $\eta = -0.5$, $\lambda^2 = 2.1944\ldots$.

and $-R$.

For the Hamiltonian system, Kivshar *et al.* find a primary $R-$*symmetric* 1-homoclinic solution for $\lambda^2 = 1.94618\ldots$, which is monotonic increasing up to its point of symmetry; see Fig. 6(a). (There are further 1-homoclinics for larger λ^2, but these will not concern us here). A simple calculation shows that $s = 1$ for this system with this reversibility, therefore only $-R$-symmetric two pulse homoclinic orbits should exist for nearby λ^2-values. One of these is plotted in fig. 6(b).

For all $\eta \in (-1, 1)$, a continuous branch of primary orbits can be traced in the (λ^2, η)-plane, graphs of which orbits do not change qualitatively. For non-zero η, we do indeed find R-symmetric two-pulse homoclinic orbits accumulating on the primary, as described by Theorems 2 and 3 (see fig. 7) for two such solutions. Figures 8 and 9 show the results of tracing out curves of the various orbits in the parameter plane. These recover both cases illustrated in fig. 1, case (a) for the $-R$-reversible two-pulses and (b) for R-reversible ones. This is in accordance with Theorem 2 and Corollary 3 with $s = 1$.

Moreover, in Tables 1 and 2, the numerical rates of accumulation of sequences of two-pulses on primary orbits are shown to agree with the scalings (12) in the Hamiltonian case $\eta = 0$ and (11) in the non-Hamiltonian case. The rates calculated from the formulae using the eigenvalues $\pm\alpha$, $\pm\omega$ calculated at $\mu = 0$ are given in the captions to the tables. Note that these eigenvalues vary with μ (which explains the numerically observed drift from the theoretical rate of accumulation for $\mu \neq 0$). A check that the computed sequence represents successive 2-pulses according to the theory is also presented in showing that the gap between the two large peaks (or troughs) differs by approximately $2\pi/\omega$.

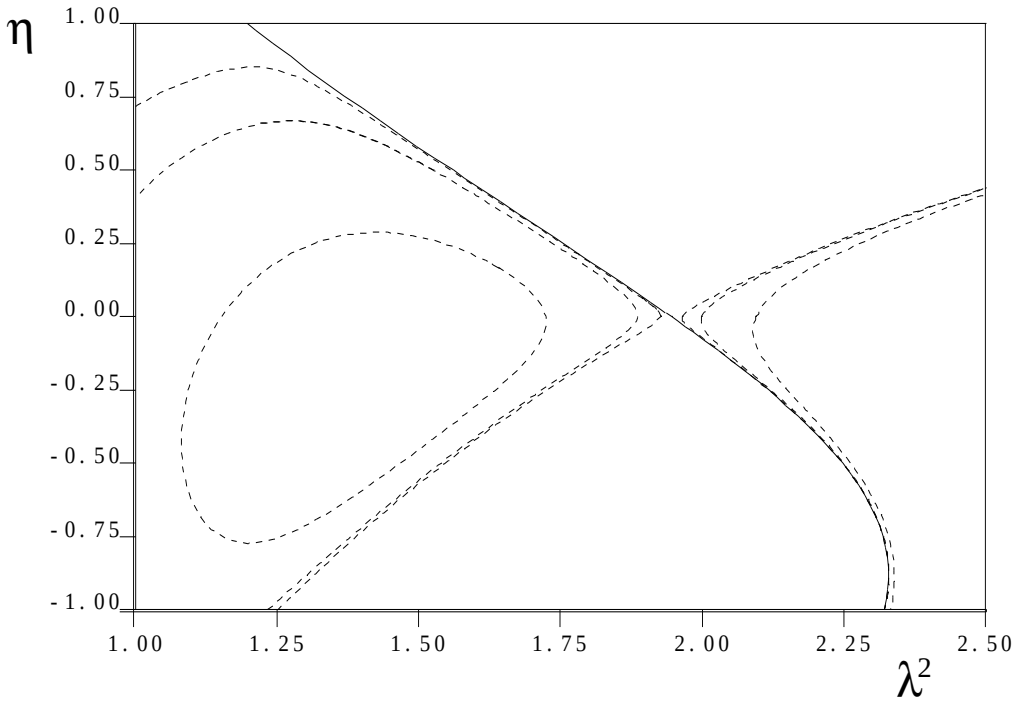

Figure 8: Bifurcation diagram in the (λ^2, η)-plane of $-R$-symmetric homoclinic orbits (dashed lines) and the primary (solid line).

$T_n - T_{n-1}$	T	λ_n^2	μ_n	μ_n/μ_{n-1}
	11.70	1.88573	-0.06045	
1.67	13.37	1.92720	-0.01898	0.3139
1.69	15.06	1.94002	-0.00615	0.3244
1.69	16.75	1.94416	-0.00202	0.3281
1.70	18.45	1.94551	-0.00067	0.3295
primary		1.94618		
1.71	18.45	1.94684	0.00066	0.3310
1.71	16.74	1.94818	0.00200	0.3324
1.71	15.03	1.95220	0.00603	0.3354
1.72	13.32	1.96415	0.01798	0.3430
1.78	11.60	1.99859	0.05241	0.3550
	9.82	2.09382	0.14764	

Table 1: Showing x-interval T between successive large maxima of $|u|$ against $\mu = \lambda^2 - 1.9461767$ for two-pulse homoclinic orbits accumulating on the primary orbit of the Hamiltonian system (13) with $\eta = 0$. The theoretical limits as $\mu \to 0$ of the first and last column respectively are $2\pi/\omega(0) = 1.6973$ and, by Equation (12) $\exp(-\alpha(0)\pi/\omega(0)) = 0.3303$.

$T_n - T_{n-1}$	T	λ_n^2	μ_n	μ_n/μ_{n-1}
(a) $-R$-symmetric				
	12.62	1.050908	-0.509751	
1.18	13.80	1.556618	-0.004042	0.00793
1.72	15.52	1.560136	-0.000523	0.12962
1.71	17.23	1.560591	-0.000069	0.13118
primary		1.560660		
(b) R-symmetric				
1.71	16.37	1.560849	0.000189	0.13205
1.73	14.66	1.562094	0.001434	0.13582
1.76	12.93	1.571219	0.010559	0.15455
1.94	11.17	1.628981	0.068321	0.19014
	9.22	1.919970	0.359310	

Table 2: Showing the x-interval T between successive large maxima of $|u|$ against $\mu = \lambda^2 - 1.56065993$ for two-pulse homoclinic orbits (both $-R$ and R-symmetric) accumulating on the primary orbit of the non-Hamiltonian system (13) with $\eta = 0.5$. The theoretical limits as $\mu \to 0$ of the first and last columns respectively are $2\pi/\omega(0) = 1.7166$ and, by Equation (11), $\exp(-2\alpha(0)\pi/\omega(0)) = 0.13140$.

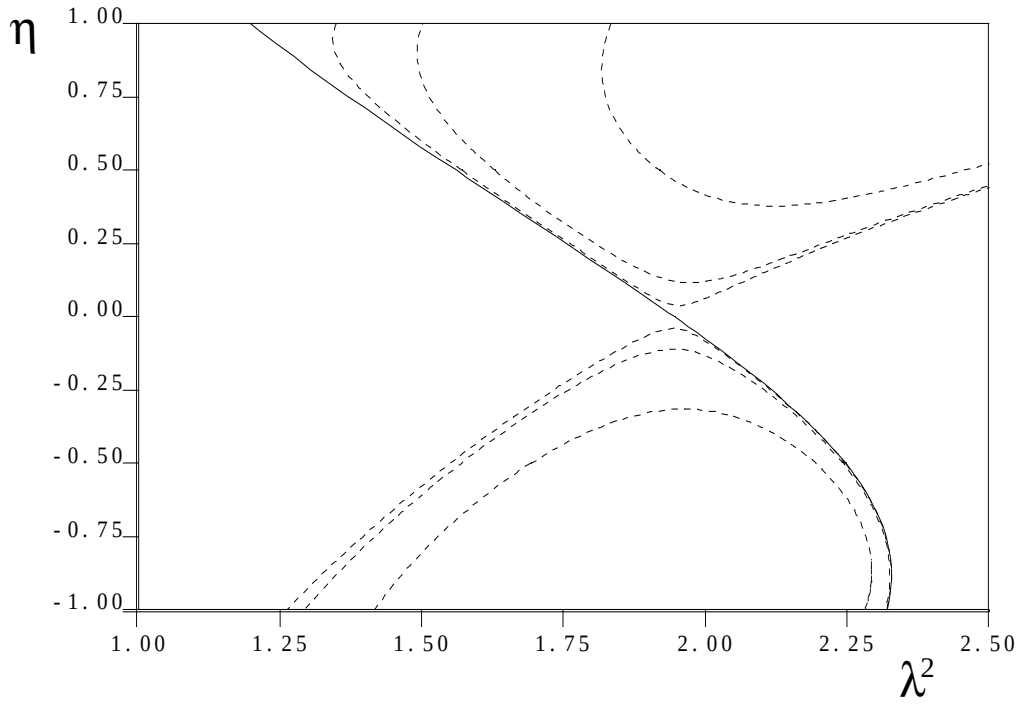

Figure 9: Bifurcation diagram in the (λ^2, η)-plane of R-symmetric homoclinic orbits (dashed lines) and the primary (solid line).

6.2 Massive Thirring Model with linear and nonlinear dispersion

A generalisation of the classical Massive Thirring Model was studied by Aceves and Wabnitz [AW89] (see also [CJ89]) as a model for an optical fibre with grating. Champneys, Malomed and Friedman [CMF98] studied the effect of dispersion on this model leading to partial differential equations of the form

$$iu_t + iu_x + Du_{xx} + \left(\sigma|u|^2 + \nu|v|^2\right) u + v = 0, \tag{14}$$

$$iv_t - iv_x + Dv_{xx} + \left(\nu|u|^2 + \sigma|v|^2\right) v + u = 0, \tag{15}$$

where $u(x,t)$ and $v(x,t)$ are complex amplitudes of two counter-propagating waves. These equations (with $\sigma = 0$) also describe stationary tunnel-coupled planar nonlinear waveguides with misaligned optical axis, t and x being the propagation distance and a transverse coordinate. Here D is an effective diffraction (rather than dispersion) coefficient.

As in [CMF98], looking for quiescent solitary waves, we substitute the ansatz, $u(x,t) = e^{-i\Omega t}U(x)$, $v = e^{-i\Omega t}V(x)$, make the further (symmetry reducing) simplification $U = V^*$ (where asterisk denotes complex conjugation) and the apply the scaling $U \to \frac{1}{\sqrt{\nu+\sigma}}U$. This results in a single second-order complex ODE which may be written in Hamiltonian form with total energy

$$H = D|U'|^2 + \Omega|U|^2 + |U|^4 + \frac{1}{2}(U^2 + (U^*)^2). \tag{16}$$

The interest in solitary waves (so called 'optical solitons') implies seeking solutions that are homoclinic to the origin.

To model the effects of nonlinear dispersion (or diffraction) we must include an extra term with coefficient β, viz

$$DU'' + iU' + \Omega U + U|U|^2 + U^* = i\beta(U|U|^2)'. \tag{17}$$

Actually this additional term in isolation is likely to be more physically meaningful for the case of the spatial waveguide model than for the temporal fibre model, because the latter would also have to take into account the so-called Raman term (see, for example [HK95]). Equation (17) may be viewed as a four-dimensional dynamical system in phase space variables $\mathrm{Re}\, U(x)$, $\mathrm{Re}\, U'(x)$, $\mathrm{Im}\, U(x)$ and $\mathrm{Im}\, U'(x)$. Viewed as such it has odd symmetry and is reversible under

$$R : (U, U') \to (U^*, -U'^*)$$

and $-R$.

In [CMF98] curves of one-pulse and two-pulse homoclinic orbits were computed in the (D,Ω)-plane for the Hamiltonian system (17) with $\beta = 0$, in the parameter region $D >$

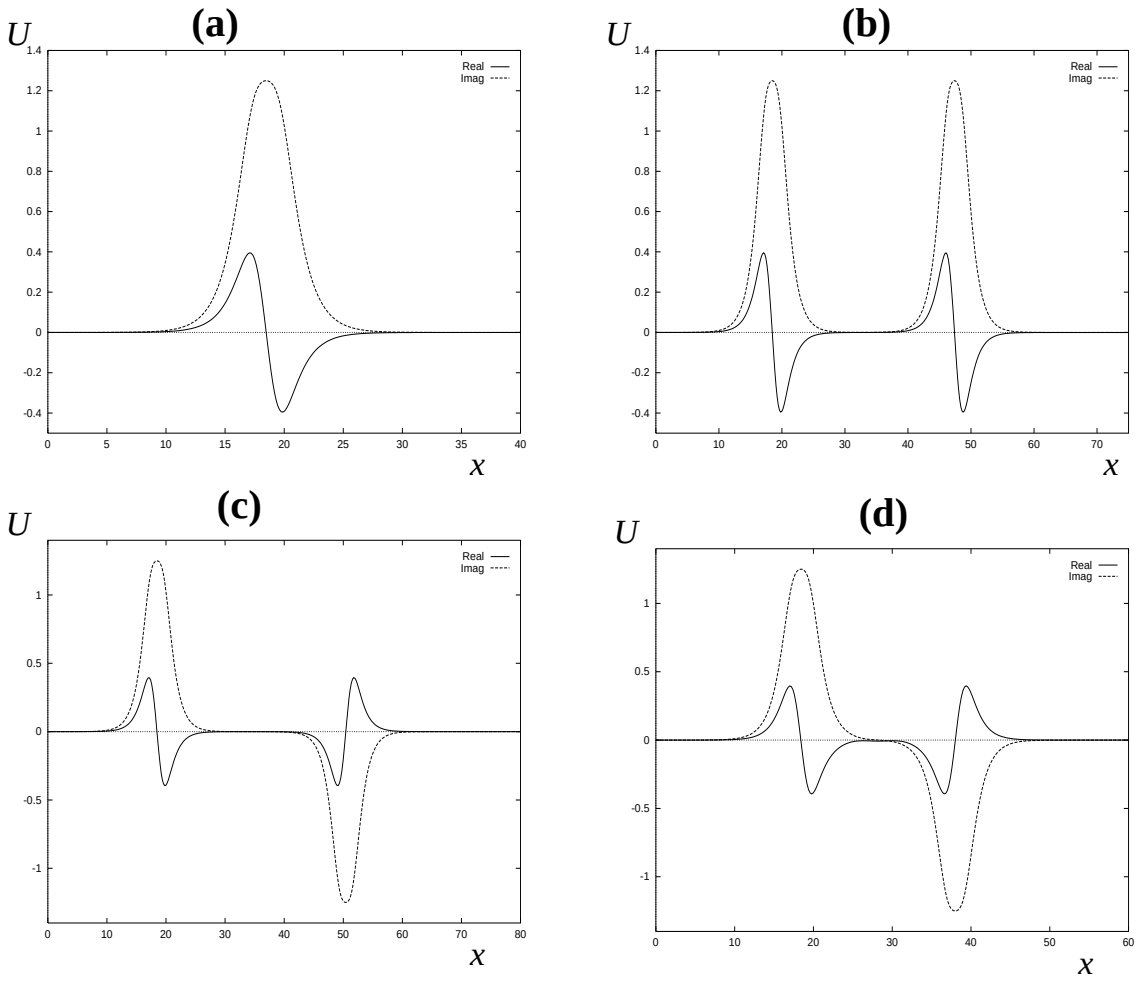

Figure 10: Homoclinic orbits of the system (17) at $\Omega = 0$ and $\beta = 0.1$. (a) primary orbit ($-R$-symmetric) for $D = 1.355173$, (b) $-R$ symmetric two-pulse for $D = 1.355187$, (c) R-symmetric two-pulse for $D = 1.355172$, and (d) R-symmetric two-pulse for $D = 1.354095$.

$T_n - T_{n-1}$	T	D_n	μ_n	μ_n/μ_{n-1}
	16.49	0.839767	-0.026258	
4.77	21.26	0.862193	-0.003832	0.1493
4.50	25.76	0.865412	-0.000613	0.1600
primary		0.8660254		
4.39	25.80	0.866633	0.000608	0.16593
4.20	21.41	0.869690	0.003664	0.17631
	17.21	0.886808	0.020783	

Table 3: Analogous to table 1, data for two-pulse $-R$-reversible homoclinic orbits for the Hamiltonian system (17) with $\beta = 0$. Here $\mu_n = D_n - 0.86660254$. The theoretical limits as $\mu \to 0$ of the first and last column respectively are $2\pi/\omega(0) = 4.442$ and, by Equation (12), $\exp(-\alpha(0)\pi/\omega(0)) = 0.1630$.

$0, |\Omega| < 1$ where the origin is a saddle centre. All solutions computed were $-R$-symmetric since a change of co-ordinates shows that $s = -1$.

Here we shall focus on showing that the addition of non-zero β destroys any Hamiltonian structure, by providing numerical evidence that Theorem 1 (specifically Corollary 3) applies. This evidence shall take the form of a sequence of R-symmetric two-pulse solutions for $\beta = 0.1$ accumulating on a one-pulse solution. Moreover we shall show that this sequence (and a sequence of $-R$ symmetric solutions) obey the scaling (11). In contrast, for the Hamiltonian system with $\beta = 0$, the scalings (12) apply.

For simplicity we take $\Omega = 0$. Our starting point is a $-R$ symmetric one-pulse homoclinic solution found by [CMF98] to occur for $\beta = 0$ at $D = \sqrt{3}/2$. A continuous branch of such solutions can be traced numerically, passing through $(D, \beta) = (1.355173, 0.1)$. Figure 10 presents, for $\beta = 0.1$, this primary orbit and some two-pulse orbits, both $-R$ *and* R-symmetric, for nearby D-values. Table 3 shows strong evidence that the two-pulses do indeed obey the accumulation law (11) whereas Table 4 shows that the two-pulses accumulating on the corresponding primary solution for $\beta = 0$ obey (12).

7 Discussion

We have demonstrated a clear distinction between the behaviour of multi-pulse homoclinic orbits to a saddle-focus equilibrium in the case of reversible and Hamiltonian systems. The

$T_n - T_{n-1}$	T	λ_n^2	μ_n	μ_n/μ_{n-1}
(a) R-symmetric				
	21.02	1.3409504	-0.0142227	
4.91	25.93	1.3550522	-0.0001209	0.0085
6.05	31.98	1.5517158	-1.51×10^{-6}	0.0124
primary		1.3551731		
(b) $-R$-symmetric				
6.09	28.99	1.3551866	1.348×10^{-5}	0.01285
5.82	22.90	1.3562225	0.0010493	0.02567
	17.08	1.3960596	0.0408865	

Table 4: Analogous to table 2, data for two-pulse homoclinic orbits for the non-Hamiltonian system (17) with $\beta = 0.1$. Here $\mu_n = D_n - 1.35517309$. The theoretical limits as $\mu \to 0$ of the first and last columns respectively are $2\pi/\omega(0) = 6.106$ and, by Equation (11), $\exp(2\alpha(0)\pi/\omega(0)) = 0.0125$.

numerical calculations provide both good qualitative and quantitative agreement with the theory. It is a subject of current interest to provide clear criteria for deciding whether there exists a change of co-ordinates to place an arbitrary reversible system in Hamiltonian form (see [LR98] for a review). So, one application of our work is a way (aided by a numerical experimentation) for deciding whether such a transformation exists in a neighbourhood of a primary homoclinic orbit to a saddle-center. If R-reversible two-pulses exist for one and only one sign of parameter perturbation from the primary orbit, then the system cannot be Hamiltonian (after any smooth co-ordinate transformation).

Despite compelling numerical evidence, we should stress that we have *not* proved rigorously that the two examples presented in Section 6 fit into the theory, as we have not proved the generic hypotheses **(H1)-(H5)**. In particular we have taken a rather restrictive assumption that there exists some smooth transformation that conjugates the system to a normal form truncated at some order. This is largely a technical assumption which is hard to verify for an arbitrary example system and does not appear necessary. The removal of this technical condition is the subject of on-going work.

References

[AW89] A. B. Aceves and S. Wabnitz. Self-induced transparency solitons in nonlinear

refractive periodic media. *Phys. Lett. A*, **141**:37-42, 1989.

[Bon97] P. Bonckaert. Conjugacy of vector fields respecting additional properties. Preprint, to appear in *Journal of Dynamical and Control Systems* 1997.

[Ch94] A. R. Champneys. Subsidiary homoclinic orbits to a saddle-focus for reversible systems. *Int. J. Bifurcation Chaos*, **4**:1447-1482, 1994.

[Ch98] A. R. Champneys. Homoclinic orbits in reversible systems and their applications in mechanics, fluids and optics. *Physica D*, **112**:158-186, 1998.

[CMF98] A. R. Champneys. Thirring solitons in the presence of dispersion. *Phys Rev Lett.* submitted September 1997.

[CJ89] D.N. Christodoulides and R.I. Joseph, Slow Bragg solitons in nonlinear periodic structures. Phys. Rev. Lett. **62**, 1746 (1989).

[De76] R. L. Devaney. Reversible diffeomorphisms and flows. *Trans. Amer. Math. Soc.*, **218**:89-113, 1976.

[Dev77] R. L. Devaney. Blue sky catastrophes in reversible and Hamiltonian systems. *Ind. Univ. Math. J.*, **26**:247–263, 1977.

[DKK91] E. Doedel, H. B. Keller and J. P. Kernevez. Numerical analysis and control of bifurcation problems. *Int. J. Bifurcation Chaos*, **1**:745-772,493-520, 1991.

[Eletal] C. Elphick, E. Tirapegui, M. E. Brachet, P. Coullet and G. Iooss. A simple global characterization for normal forms of singular vector fields. *Physica D*, **29**:95–127, 1987.

[FT96] B. Fiedler and D. Turaev. Coalescence of reversible homoclinic orbits causes elliptic resonance. *Int. J. Bifurcation Chaos*, **6**:1007-1027, 1996.

[Här93] J. Härterich. *Kaskaden homokliner Orbits in reversiblen dynamischen Systemen.* Masters' Thesis Universität Stuttgart, 1993. English translation appeared as "Cascades of reversible homoclinic orbits to a saddle-focus equilibrium" **Physica D 112** 187-200 1998.

[Har82] P. Hartman. *Ordinary Differential Equations.* Birkhäuser Verlag, Boston, 2nd edition, 1982.

[HK95] A. Kodama and A. Hasegawa. *Solitons in optical communications.* Clarendon Press, Oxford, 1995.

[IA92] G. Iooss and M. Adelmeyer. *Topics in Bifurcation Theory and Applications*, volume **3** of *Adv. Series in Nonlinear Dynamics*. World Scientific, 1992.

[KCCB97] Yu. Kivshar, A. R. Champneys, D. Cai and A. R. Bishop Bound states of intrinsic localized modes. In preparation 1997.

[Kno97] J. Knobloch. Bifurcation of degenerate homoclinics in reversible and conservative systems. *J. Dynamics Diff. Eqns.*, 1997

[KL95] Yu. O. Koltsova and L. M. Lerman. Periodic orbits and homoclinic orbits in a two-parameter unfolding of a HHamiltonian system with a homoclinic orbit to a saddle-centre. *Int. J. Bifurcation Chaos*, **5**:397-408, 1995.

[LR98] J. S. W. Lamb and J. A. .G. Roberts. Time reversal symmetry in dynamical systems: an overview. *Physica D*, **112**:1-39, 1998.

[Ler91] L. M. Lerman. Complex dynamics and bifurcations in a Hamiltonian system having a transversal homoclinic orbit to a saddle focus. *Chaos*, **1**:174-180, 1991.

[MHO92] A. Mielke, P. Holmes, and O. O'Reilly. Cascades of homoclinic orbits to, and chaos near, a Hamiltonian saddle-center. *J. Dyn. Diff. Equ.*, **4**:95–126, 1992.

[Reg97] C.G. Ragazzo. Irregular dynamics and homoclinic orbits to Hamiltonian saddle centers. *Comm. Pure Appl. Math.* **50**:105-147, 1997.

[Sam83] V. S. Samovol, Equivalence of systems of differential equations in a neighborhood of a singular point. *Trans. Moscow Math. Soc.* **44**:217-237, 1983.

[San95] Sandstede, B. Center manifolds for homoclinic solutions. WeierstraßInstitut für Angewandte Analysis und Stochastik *Preprint* No. 186, 1997.

[Saetal96] B. Sandstede, C. K. R. T. Jones and J.C. Alexander. Existence and stability of N-pulses on optical fibres with phase-sensative amplifiers. *Physica D*, **106**:167-206, 1997.

[VF92] A. Vanderbauwhede and B. Fiedler. Homoclinic period blow-up in reversible and conservative systems. *Z. angew. Math. Phys.*, **43**:292–318, 1992.